Model-Based Shared Control of a Hybrid FES-Exoskeleton: an Application in Participant-Specific Robotic Rehabilitation

Hossein Kavianirad[1] Moein Forouhar[2] Hamid Sadeghian[2] Satoshi Endo[1] Sami Haddadin[2] Sandra Hirche[1]

2023 International Conference on Rehabilitation Robotics (ICORR) | 979-8-3503-4275-8/23/$31.00 ©2023 IEEE | DOI: 10.1109/ICORR58425.2023.10304764

***Abstract*— Hybrid exoskeleton, comprising an exoskeleton interfaced with functional electrical stimulation (FES) technique, is conceptualized to complement the weakness of each other in automated neuro-rehabilitation of sensory-motor deficits. The externally actuating exoskeleton cannot directly influence neurophysiology of the patients, while FES is difficult to use in functional or goal-oriented tasks. The latter challenge is largely inherited from the fact that the dynamics of the muscular response to FES is complex, and it is highly user- and state-dependent. Due to the retardation of the muscular contraction response to the FES profile, furthermore, a commonly used model-free control scheme, such as PID control, suffers performance. The challenge in FES control is exacerbated especially in the presence of the actuation redundancy between the volitional activity of the user, powered exoskeleton, and FES-induced muscle contractions. This study therefore presents trajectory tracking performance of the hybrid exoskeleton in a novel model-based hybrid exoskeleton scheme which entices user-specific FES model-predictive control.**

***Index Terms*— Hybrid exoskeleton, functional electrical stimulation, cooperative control, impedance control, rehabilitation**

I. Introduction

Damage to the central nervous system following spinal cord injuries (SCI) or stroke may cause a loss of function in the upper limb. In order to improve the motor control of the patients through neural rehabilitation, various actuation techniques have been introduced. For instance, functional electrical stimulation (FES) uses electrical stimulation to actively induce muscle contraction. Despite the fact that there is evidence of neuroplasticity following long-term FES exposure [1], control of the muscle contractions through stimulation with a surface electrode is imprecise for assisting goal-oriented tasks. Furthermore, the stimulation accelerates muscle fatigue which further deteriorates control performance of the system [2]. Exoskeletons, on the other hand, can augment smooth and precise motion coupled with the patient's residual motion. However, the motions are externally guided, and the exercise is often ineffective unless patients are actively engaged [3]. Hybrid exoskeleton can overcome the drawbacks of these actuators [4]–[6], and it is a promising approach to improve the recovery of human motor functions without introducing excessive muscle fatigue [7], [8]. However, combining FES and exoskeleton for assisting limb movement poses various challenges. From control perspectives, for instance, there is an actuation redundancy problem [9]–[11], such that the effect of human volitional activities must be considered in the control loop [12], as well as the coordination between the exoskeleton and FES actuations. Furthermore, FES is directly interfaced with the user, and participant-specific behavior must be considered at the neuromachanical level for control performance [8], [13].

Various theoretically and empirically motivated hybrid exoskeleton control methods address these challenges [8], [11]. [8], for example, presents a theoretical cooperative control approach based on muscle-model using inverse dynamics optimization to allocate the control effort between the two actuators in the lower-limb motion. Although the proposed method is based on participant-specific neurophysiological muscle-model, the effect of the human volitional activities is not considered. In contrast, [11] proposes the shared control of elbow movements based on optimization which minimizes a cost function consisting of trajectory tracking error, control inputs of two actuators, and time derivative of the control inputs. However, , no dynamics is considered for the torque-FES model in the low-level control scheme, and only a static map of torque is considered as a function of FES pulse-width and elbow angle, as described in [14], [15].

In this study, we present a user-specific control architecture which considers human volitional activities, actuator redundancy, torque-exoskeleton model, and participant-specific torque-FES model. On the high-level control, shared control deals with the model and environment uncertainties while considering the volitional human effort in the control loop. Cooperative control then distributes the control effort between the exoskeleton and FES. On the low-level torque-FES control, activation and contraction dynamics are taken into account, and model-predictive control (MPC) is used for tracking desired trajectory.

II. Hybrid control scheme

A. Shared and cooperative control

Augmenting FES and an exoskeleton with a human in the loop as illustrated in Fig. 1 rises a question on the control effort distribution. The high-level control architecture comprises shared and cooperative control which enable effective distribution of the control efforts between the exoskeleton and FES, while adapting to the human effort (see. Fig. 2). In order to robustify against the model and environment uncertainties, and to consider the volitional human effort in

[1] Chair of Information-oriented Control-School of Computation, Information and Technology, Technical University of Munich, 80992 Munich, Germany. E-mails: {hossein.kavianirad, s.endo, hirche}@tum.de.

[2] Munich Institute of Robotics and Machine Intelligence, Technical University of Munich, 80992 Munich, Germany. H. Sadeghian also has an affiliation with the University of Isfahan, Isfahan, Iran. E-mails: {moein.forouhar, hamid.sadeghian, haddadin}@tum.de.

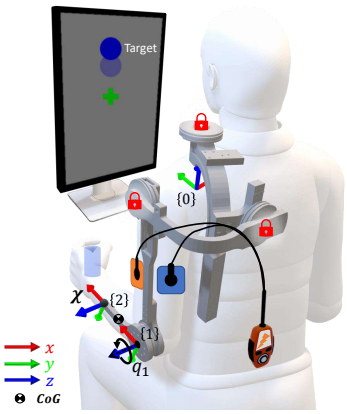

Fig. 1. Illustration of the hybrid exoskeleton. In a tracking task, a participant follows a target on a computer screen by flexing and extending the elbow. In the study, the shoulder joints are locked and the FES stimulation is applied to the elbow extensor (triceps brachii) and flexor (brachialis). The $\{0\}$, $\{1\}$, and $\{2\}$ frames belong to the fixed, elbow, and F/T sensor, respectively.

the control loop, we employ a shared control framework with a reference impedance model which derives torque necessary for the system to minimize the tracking error. The cooperative control then distributes the control effort, i.e. the desired torque, between the available actuators, i.e. FES and exoskeleton as

$$\begin{aligned} \tau_d^{FES} &= \alpha \tau_d \\ \tau_d^{EXO} &= (1-\alpha)\tau_d \ , \end{aligned} \tag{1}$$

where α is the cooperative gain and τ_d, τ_d^{FES}, τ_d^{EXO} are total, FES, and exoskeleton desired torque, respectively. In order to focus the analyses on the performance of the FES control methods, the effort allocation between the exoskeleton and FES in this study is fixed ($\alpha = 0.25$).

B. FES control

The neuromuscular response to FES is participant-specific, and is subject to a function of various complex and time-varying factors [16]. Therefore, to control the neuromuscular system with FES, we first develop the participant-specific FES-torque model. Then, we use this model for the hybrid control scheme.

1) FES-torque model: Various physiological and empirical models describing the response of skeletal muscle to electrical stimulation are found in literature [17]–[19]. For the FES-torque model, we consider the model consists of activation and contraction dynamics [19]. The active torque of FES-induced muscle contraction, τ^{FES}, is the product of contraction dynamics and activation dynamics. Fig. 3 illustrates the FES-torque model considered in this work. In this model, the contraction dynamics is considered as the maximum torque which can be produced at each angle of the (elbow) joint, $\tau_{max}(\theta)$, and the activation, a_{act}, determines the point to which a motion unit is recruited by FES;

$$\tau^{FES} = \tau_{max}(\theta) a_{act} \ . \tag{2}$$

Based on [8], [19], [20], the following second-order dynamics , encompassing the activation dynamics and calcium dynamics, formulates the excitation of artificially stimulated muscles.

$$\dot{a} = Aa + Ba_r \ , \tag{3}$$

where $a = [a_{act}, \dot{a}_{act}]^T$, A and B are 2×2 and 2×1 unknown matrices describing activation dynamics. a_r is the recruitment characteristic which shows the relationship between the FES intensity and the percentage of the motor unit activated by FES, formulated as

$$a_r = G(u_n, \theta) \ , \tag{4}$$

where u_n is normalized FES intensity and G is nonlinear recruitment curve [11], [15], [19]. The static maps $\tau_{max}(\theta)$ and $G(u_n, \theta)$, as well as the dynamic maps A and B are unknown and participant-specific, therefore necessary to learn on each person.

2) FES torque control: The low-level control scheme for FES-torque control consists of model-based FES control using neuromuscular dynamics (Fig. 3), defined as (2)-(4) and PID control. This scheme illustrates a cohesive case which includes both model-based and PID control. The respective control requires different inputs and is singly introduced into the scheme by a switch (Fig. 4). Participant-specific learned models of the static ($\tau_{max}(\theta)$, $G(u_n, \theta)$) and dynamics (A, B) maps, desired FES torque (τ_d^{FES}), measured interaction torque (τ) and elbow angle (θ) are the inputs of MPC-based FES control. Given (2), a_{act} can be determined based on measured and desired FES torque. By the definition of the activation dynamics (3) and using MPC which minimizes the tracking error, a_r is determined based on a_{act}. To normalize the FES intensity from recruitment characteristic a_r, solution of static map (4) is necessary, and this is achieved by minimizing the cost function $J = (G(u_n, \theta) - a_r)^2$,

$$\begin{aligned} u_n^{FES\star} &= \arg\min_{u_n^{FES}} J(u_n, \theta, a_r) \\ s.t. \quad & 0 \le u_n^{FES} \le 1 \ . \end{aligned} \tag{5}$$

Finally, the FES intensity can be determined based on participant-specific parameters, u_{min} and u_{max}, and model-based and PID controller outputs, u_n^{FES} and $u_{n,pid}^{FES}$, respectively;

$$u^{FES} = u_{min} + (u_{max} - u_{min})(u_n^{FES} + u_{n,pid}^{FES}) \ . \tag{6}$$

C. Exoskeleton control

The cooperative control system commands a desired torque applied to the human arm by the exoskeleton. However, due to the presence of friction in the system caused by the use of a Bowden cable for remote actuation [21] and the weight of the forearm and exoskeleton link, it is necessary to compensate for them. To mitigate these factors, the following torque command is sent to the low-level torque controller;

$$\tau^{EXO} = \tau_d^{EXO} + \tau_g + \tau_f \ , \tag{7}$$

where τ_g denotes the gravity torque to compensate the weight of the participant's forearm and the last link of the

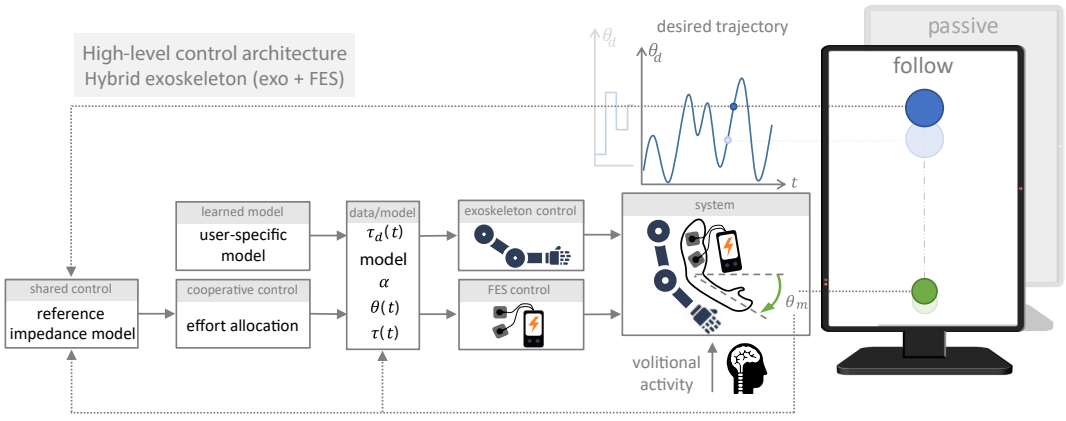

Fig. 2. The high-level control architecture of the hybrid exoskeleton, including shared, cooperative, FES-torque, and exo-torque control.

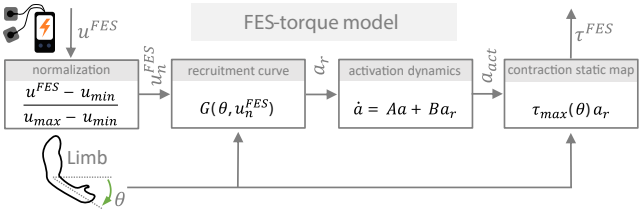

Fig. 3. The FES-torque model consists of activation and contraction dynamics of muscles in response to FES.

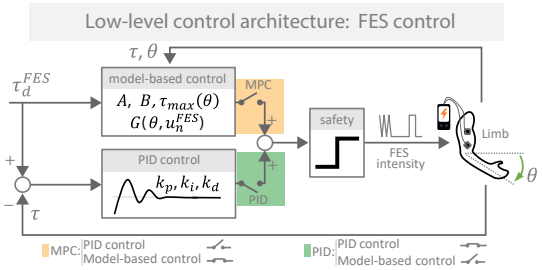

Fig. 4. The low-level FES-torque control architecture, including both model-based and PID FES-torque control. A selection of PID or model-based control (here MPC) is modulated by a switch.

exoskeleton. τ_f compensates the friction of the exoskeleton joints as well as that of the Bowden cable. In order to estimate the friction torque, one of the effective methods is to use a momentum observer [22]. The momentum observer given by (8) is employed to obtain the residual $\zeta(t)$. In this equation, k_I represents the observer gain, $p(t)$ denotes the momentum of the combination of the forearm and the last link,

$$\zeta(t) = k_I \left[p(t) - \int_0^t \left(\tau^{EXO} - \tau_g + \zeta(\sigma) \right) d\sigma \right] \tag{8}$$

$$\dot{\zeta} = -k_I \zeta - k_I \left(\tau_e + \tau_f \right) \ . \tag{9}$$

The residual $\zeta(t)$ estimates the amount of friction torque in the system. However, the residual converges to the sum of $(\tau_f + \tau_e)$ which represents the total external torque acting on the system, due to external torques applied by the arm, τ_e, and friction. Using the measurement of a force-torque (F/T) sensor embedded at the contact point, one can obtain the friction torque by subtracting the external torque from the residual value. This estimation is then inserted in (7).

III. Experimental Evaluation

A. Participants

Five healthy individuals participated (four males and one female) in this study. All the participants were right-handed and performed the task with their left hand due to the exoskeleton construction. Table I summarizes their demographic data. Prior to their participation, all the participants gave informed consent.

TABLE I
PARTICIPANT DEMOGRAPHICS

Participant	Gender	Age (years)	EXO.*	FES*
1	Male	29	Yes	Yes
2	Male	31	Yes	No
3	Male	24	No	No
4	Female	33	No	No
5	Male	33	Yes	No

* previous experience with an exoskeleton and FES

B. Apparatus

1) Functional electrical stimulation: A research-grade FES device (Tecnalia Research & Innovation, Spain) is interfaced with a custom-designed multi-array electrode. The module allows online control of stimulation parameters, including the pulse width, intensity, and frequency of stimulation. In this study, varying stimulation intensity with the 25 Hz biphasic electrical pulse and precision of 100 μA is considered as a control variable. The cathode electrodes are placed along the upper arm girth, and the anode electrodes are placed near the distal base of the biceps brachii and triceps bracii for inducing elbow flexion and extension, respectively. Rubber band fixtures are used to ensure the contact between the electrode and the skin. The lower and upper saturation limits of the stimulation intensities (u_{min} and u_{max}) are respectively set to each participant's motor

threshold and maximum comfort as collected prior to the study.

2) Exoskeleton: The exoskeleton is attached with a properly designed mechanical interface to the forearm of the participant. A nano-25 F/T sensor (ATI Industrial Automation, USA) is placed at this interface between the exoskeleton and the user's wrist to measure interaction torque as illustrated in Fig. 5. The exoskeleton is run on a computer with real-time Ubuntu kernel which communicates the sensors and desirable torque data with another computer running the cooperative and shared control module and FES device via UDP connection. The desired exoskeleton torque is received from this module, and then superimposed onto the gravity/friction compensation torque by (7). To measure the weight of the combination of the participant's forearm and exoskeleton link, we ask the participant to hold their arm in a relaxed position while it is attached to the exoskeleton at 0° elbow angle. The degree is defined so 0°corresponds to the neutral angle in terms of flexion/extension, and the forearm is parallel to the ground as the upperarm naturally points downwards in a sitting posture. The system then measures the average value of the end-effector link torque sensor for 5 seconds. For other angles, we calculate the weight by multiplying this value by the cosine of the angle.

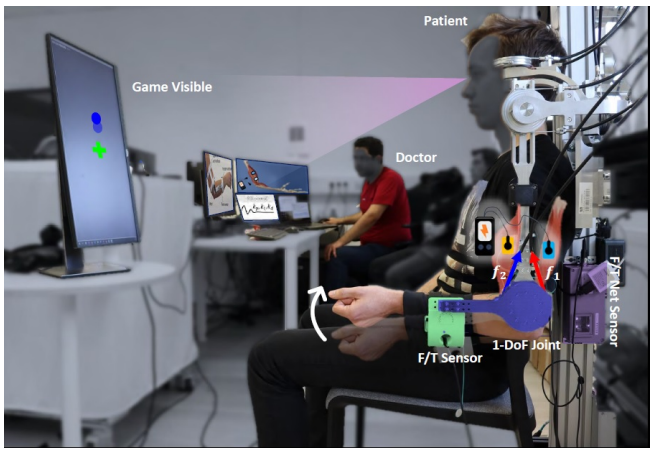

Fig. 5. Hybrid exoskeleton system with a participant performing the tracking task. The system comprises an upper limb exoskeleton, providing assistance for arm movement, and FES applied to the participant's elbow muscles to assist the task.

C. Experimental Design

The study evaluates advantages of our FES-torque model in the hybrid exoskeleton control scheme. Therefore, an MPC performance is contrasted with a PID control as well as a shame FES stimulation below the FES motor threshold. As performance measures with assisted devices are often saturated with healthy participants, the study design systematically varies the involvement of the participants, such that they are instructed to either actively follow a target or remain passive throughout a trial. Furthermore, to quantify the additive benefit of the exoskeleton, we compared the FES performance with or without the exoskeleton. To sum, the study is a 3-way within-subject design where we varied the FES control scheme (MPC vs. PID vs. shame), exoskeleton assistance (active vs. inactive), and user involvement (active vs. passive). Given the combination of sham FES, inactive exoskeleton, and passive user encompasses no actuation in the setup, there are 11 total experimental conditions. The participants performed these conditions in a random order. In each condition, the participant tracked a sinusoidal reference trajectory, θ_d, on a computer display, generated as (10);

$$\theta_d = 30^\circ sin(\frac{2\pi(t-t_0)}{10}) sin(\frac{2\pi(t-t_0)}{5.3775}) \\ 0 \leq t \leq 60, \;\; t_0 : \; random \; offset \; . \tag{10}$$

Each trial lasted for 60 seconds as denoted by t, and a random time-offset (t_0) is given to disrupt prediction of the trajectory by the user.

D. Procedure

First, the exoskeleton and the FES system are fitted to each participant (Fig. 5), and a calibration of the exoskeleton and FES is performed before the tracking task commence. Calibration is required for the generation of FES stimulation profiles and the gravity compensation of the exoskeleton. A participant sits on the chair and is asked to remain passive in the arm. The FES calibration starts with manually adjusting the stimulation intensity to find the maximum-but-comfortable intensity threshold and minimum threshold which provokes contractions of the targeted muscles (elbow flexor/extensor). Then, the weight of the arm resting on the exoskeleton is measured on the exoskeleton and then applied to the gravity compensation by the exoskeleton. Subsequently, the FES-torque map, (2) to (4), is generated by administering different FES intensities at various elbow angles. The joint torque resulted from five different FES intensities (equally spaced between maximum and minimum intensities) at three elbow angles (-20°, 0°, and +20°) is analyzed in a random sequence for flexsor and extensor elbow motions each. The joint angle is guided and the measurement of induced torque is made by the exoskeleton. Each stimulation lasts 5 seconds, interleaved with 5 seconds of a resting period. Given the FES profile, the elbow angle and the resulted torque, the user-specific nonlinear recruitment curve (4) is modeled by the cubic spline. The linear activation dynamics (3) is then learnt using the linear regression method for the MPC-based FES control. During the tracking task, the participants are instructed to move their elbow to follow a target that appeared on the screen as accurately as possible. For the passive conditions, the participants are asked to relax. All instructions are given on the computer display.

IV. Results

Fig. 6 illustrates an exemplar performance of PID- and MPC-based FES control when the exoskeleton assisted the active participant. The tracking performance of the controllers are compared by means of the root mean square error (RMSE) between the target trajectory, θ_d, and the

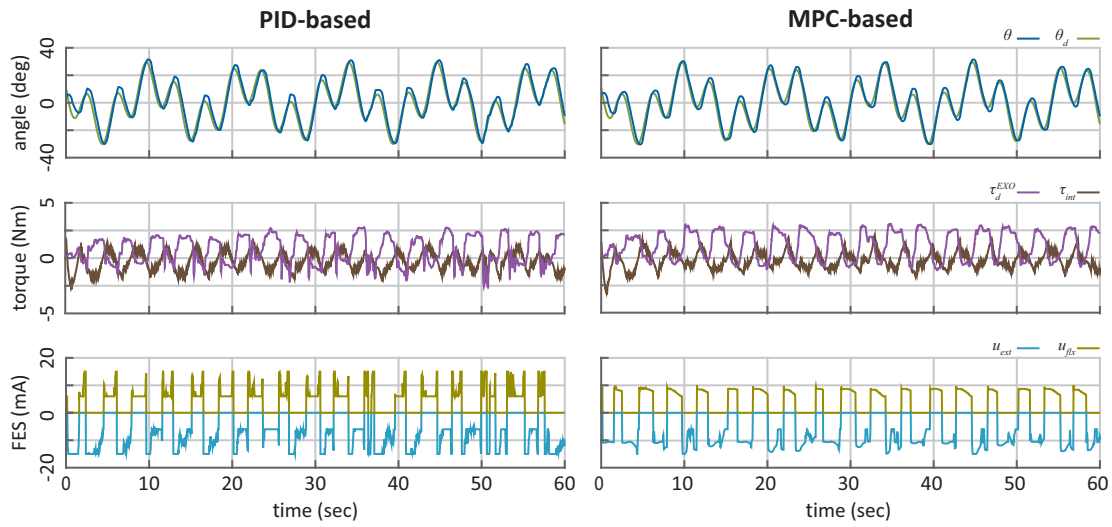

Fig. 6. Comparison of PID- and MPC-based FES control in active exoskeleton. This figure shows the desirable and measured elbow angle (θ and θ_d), assistive elbow torque by the exoskeleton (τ_d^{EXO}), measured interaction torque (τ_{int}), and flexion/extension of FES control profiles. Both PID- and MPC-based controllers demonstrated comparable tracking performance, likely due to the presence of the exoskeleton assistance. Notably, however, the MPC derives a smoother FES profile.

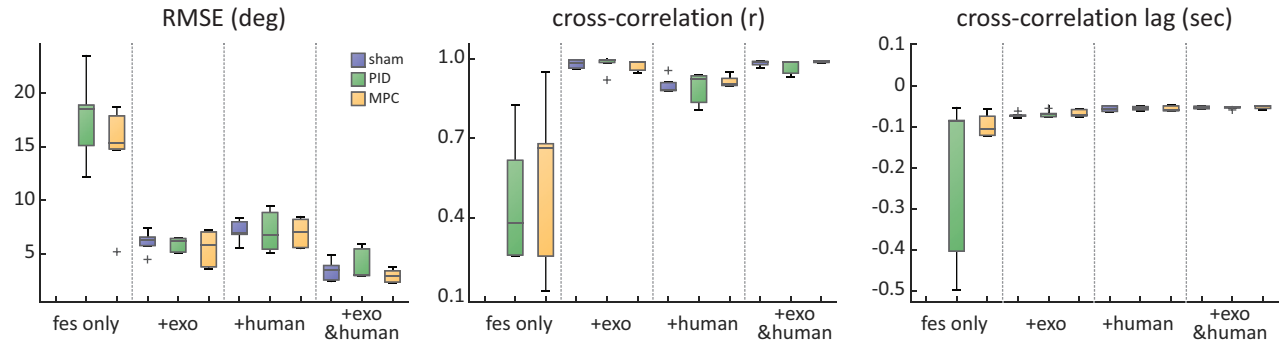

Fig. 7. The box and whisker plots of the dependent variables. The error bars represent the 1.5 interquartile range. Accuracy of the different FES control methods (sham, PID, and MPC FES control) are contrasted across the hybrid control scenarios (*+exo*: active exoskeleton, *+human*: active participant). No result is presented for "sham-FES" only as there was no actuation in place. Negative lag of the cross-correlation function indicates the tracking of the participant lagged behind the reference trajectory.

measured elbow angle, θ. Furthermore, the temporal dependency of the tracking performance was quantified with the maximum of the cross-correlation function between these two profiles. Due to the small sample-size of the present study, the median (M) and the interquartile range (IQR) are reported. Moreover, to compare the effects of the FES control scheme on the results, nonparametric statistical Friedman's test is conducted. Fig. 7 summarizes RMSE and the cross-correction analysis across the experimental conditions. In general, RMSE was the highest ($M = 15.01°$, $IQR = 3.43°$) when the FES was the only actuator (*fes only*). The presence of the active human participants (*+human*) lowered RMSE ($6.96°$, $1.31°$). Further reduction in RMSE was found in the presence of the exoskeleton assistance, especially in the hybrid case with the active human participation (*+exo&human*) ($3.04°$, $1.02°$). Although the Friedman's test does not show difference in RMSE across the FES control methods ($\chi^2(2) = 0.99$, $p = 0.55$), the smallest RMSE was reported from the MPC ($5.81°$, $4.27°$), followed by PID control ($6.42°$, $5.74°$), and sham FES stimulation ($6.68°$, $6.61°$). The analysis of cross-correlation coefficients also found a similar trend, such that the presence of the active human participants and/or the exoskeleton attenuated the correlation coefficients, but higher coefficients in the MPC (0.66, 0.24) are accentuated in comparison to the PID control (0.38, 0.40) when FES was the only actuator. The Friedman's test confirms statistical significance of this difference ($\chi^2(2) = 6.19, p = 0.022$) Furthermore, this interpretation is supported from the perspective of the correlation lag ($\chi^2(2) = 4.05$, $p = 0.019$).

V. Discussions and Conclusion

The present study demonstrated utility of a model-based FES control in a shared and cooperative control architecture for an upper-body hybrid exoskeleton. In general, our MPC for FES showed improvements over model-free control (i.e. PID) in particular with temporal coordination quantified by the cross-correlation function. Close inspection of the

FES profiles indicated our MPC-based method generated smoother FES profiles, assumingly resonating the slow dynamics of the muscles more appropriately than the PID-based control. Although further test is necessary, it is likely that our MPC-based method more efficiently recruits muscles for goal-oriented tasks, and it can be beneficial for not only a task performance, but a longer-term use against muscle fatigue. In order to better control the effects of FES control methods, the present study used the effort allocation between the exoskeleton and FES was fixed. Our model-based shared control opens new opportunities to extend how the system efforts could be distributed from the performance as well as the neuromechanical perspectives to induce different control strategies as a future work.

In conclusion, this paper presents a novel model-based participant-specific shared control based on activation and contraction dynamics for hybrid rehabilitation applications. The high-level control, composed of shared and cooperative control, allows the efficient combination of FES, exoskeleton, and volitional activity of the human in performing the rehabilitation tasks. The control architecture with model-based FES control (MPC with contraction and activation dynamics) shows superior tacking performance in comparison with PID-based FES control hybrid FES-exoskeleton control as well as in solo FES control.

VI. ACKNOWLEDGMENT

The presented work was supported by the Horizon 2020 research and innovation program of the European Union under grant agreement no. 871767 of the project ReHyb, and the European Research Council (ERC) Consolidator Grant "Safe data-driven control for human-centric systems (CO-MAN)" under grant agreement number 864686. We gratefully acknowledge the funding of the Lighthouse Initiative Geriatronics by LongLeif GaPa gGmbH (Project Y) and financial support by the Federal Ministry of Education and Research of Germany (BMBF) in the programme of "Souverän. Digital. Vernetzt." Joint project 6G-life, project identification number 16KISK002.

REFERENCES

[1] D. B. Popovic, M. B. Popovic, T. Sinkjær, A. Stefanovic, and L. Schwirtlich, "Therapy of paretic arm in hemiplegic subjects augmented with a neural prosthesis: a cross-over study," *Canadian journal of physiology and pharmacology*, vol. 82, no. 8-9, pp. 749–756, 2004.

[2] N. Dunkelberger, E. M. Schearer, and M. K. O'Malley, "A review of methods for achieving upper limb movement following spinal cord injury through hybrid muscle stimulation and robotic assistance," *Experimental Neurology*, vol. 328, 2020.

[3] L. Marchal-Crespo and D. J. Reinkensmeyer, "Review of control strategies for robotic movement training after neurologic injury," *Journal of NeuroEngineering and Rehabilitation*, vol. 6, pp. 1–15, 6 2009.

[4] N. A. Kirsch, X. Bao, N. A. Alibeji, B. E. Dicianno, and N. Sharma, "Model-based dynamic control allocation in a hybrid neuroprosthesis," *IEEE Transactions on Neural Systems and Rehabilitation Engineering*, vol. 26, no. 1, pp. 224–232, 2018.

[5] D. Wolf, N. Dunkelberger, C. G. McDonald, K. Rudy, C. Beck, M. K. O'Malley, and E. Schearer, "Combining functional electrical stimulation and a powered exoskeleton to control elbow flexion," in *2017 International Symposium on Wearable Robotics and Rehabilitation (WeRob)*, 2017, pp. 1–2.

[6] A. S. Gorgey, C. D. Black, C. P. Elder, and G. A. Dudley, "Effects of electrical stimulation parameters on fatigue in skeletal muscle," *journal of orthopaedic & sports physical therapy*, vol. 39, no. 9, pp. 684–692, 2009.

[7] A. M. Stewart, C. G. Pretty, M. Adams, and X. Chen, "Review of upper limb hybrid exoskeletons," *IFAC-PapersOnLine*, vol. 50, no. 1, pp. 15 169–15 178, 2017.

[8] F. Romero-Sánchez, J. Bermejo-García, J. Barrios-Muriel, and F. J. Alonso, "Design of the cooperative actuation in hybrid orthoses: a theoretical approach based on muscle models," *Frontiers in neurorobotics*, vol. 13, p. 58, 2019.

[9] N. Kirsch, N. Alibeji, B. E. Dicianno, and N. Sharma, "Switching control of functional electrical stimulation and motor assist for muscle fatigue compensation," in *2016 American Control Conference (ACC)*. IEEE, 2016, pp. 4865–4870.

[10] E. Bardi, S. Dalla Gasperina, A. Pedrocchi, and E. Ambrosini, "Adaptive cooperative control for hybrid fes-robotic upper limb devices: a simulation study," in *2021 43rd Annual International Conference of the IEEE Engineering in Medicine & Biology Society (EMBC)*. IEEE, 2021, pp. 6398–6401.

[11] N. Dunkelberger, S. A. Carlson, J. Berning, K. C. Stovicek, E. M. Schearer, and M. K. O'Malley, "Shared control of elbow movements with functional electrical stimulation and exoskeleton assistance," in *2022 International Conference on Rehabilitation Robotics (ICORR)*. IEEE, 2022, pp. 1–6.

[12] H. Kavianirad, S. Endo, T. Keller, and S. Hirche, "Emg-based volitional torque estimation in functional electrical stimulation control," in *The 7th IEEE-EMBS Conference on Biomedical Engineering and Sciences (IECBES 2022)*, 2022.

[13] C.-H. Chang, V. H. Duenas, and A. Sanyal, "Model free nonlinear control with finite-time estimation applied to closed-loop electrical stimulation induced cycling," in *2020 American Control Conference (ACC)*. IEEE, 2020, pp. 5182–5187.

[14] W. K. Durfee and K. E. MACLean, "Methods for estimating isometric recruitment curves of electrically stimulated muscle," *IEEE Transactions on Biomedical Engineering*, vol. 36, no. 7, pp. 654–667, 1989.

[15] D. N. Wolf, Z. A. Hall, and E. M. Schearer, "Model learning for control of a paralyzed human arm with functional electrical stimulation," in *2020 IEEE International Conference on Robotics and Automation (ICRA)*. IEEE, 2020, pp. 10 148–10 154.

[16] A. Sena, H. Kavianirad, S. Endo, E. Burdet, and S. Hirche, "The gap in functional electrical stimulation simulation," in *3rd Workshop on Closing the Reality Gap in Sim2Real Transfer for Robotics*, 2022.

[17] C. A. Cousin, V. H. Duenas, C. A. Rouse, and W. E. Dixon, "Admittance trajectory tracking using a challenge-based rehabilitation robot with functional electrical stimulation," in *2018 Annual American Control Conference (ACC)*. IEEE, 2018, pp. 3732–3737.

[18] N. A. Alibeji, V. Molazadeh, B. E. Dicianno, and N. Sharma, "A control scheme that uses dynamic postural synergies to coordinate a hybrid walking neuroprosthesis: Theory and experiments," *Frontiers in neuroscience*, vol. 12, p. 159, 2018.

[19] Y. Chen, J. Hu, L. Peng, and Z.-g. Hou, "The fes-assisted control for a lower limb rehabilitation robot: simulation and experiment," *Robotics and Biomimetics*, vol. 1, no. 1, p. 2, 2014.

[20] M. Gföhler, T. Angeli, and P. Lugner, "Modeling of artificially activated muscle and application to fes cycling," *Journal of Mechanics in Medicine and Biology*, vol. 4, no. 01, pp. 77–92, 2004.

[21] A. Toedtheide, X. Chen, H. Sadeghian, N. Abdeldjallil, and S. Haddadin, "A force-sensitive exoskeleton for teleoperation: An application in elderly care robotics," in *2023 IEEE International Conference on Robotics and Automation (ICRA)*. IEEE, 2023.

[22] A. De Luca, A. Albu-Schaffer, S. Haddadin, and G. Hirzinger, "Collision detection and safe reaction with the dlr-iii lightweight manipulator arm," in *2006 IEEE/RSJ International Conference on Intelligent Robots and Systems*. IEEE, 2006, pp. 1623–1630.